(This is a sample cover image for this issue. The actual cover is not yet available at this time.)

Journal of Non-Newtonian Fluid Mechanics 191 (2013) 25–34

Contents lists available at SciVerse ScienceDirect

Journal of Non-Newtonian Fluid Mechanics

journal homepage: http://www.elsevier.com/locate/jnnfm

Simulations of mobilization of Bingham layers in a turbulently agitated tank

J.J. Derksen

Chemical & Materials Engineering, University of Alberta, Edmonton, Alberta, Canada T6G 2G6

ARTICLE INFO

Article history:
Received 26 August 2012
Received in revised form 19 September 2012
Accepted 21 September 2012
Available online 19 November 2012

Keywords:
Mixing
Blending
Bingham liquid
Yield stress
Buoyancy
Lattice-Boltzmann method

ABSTRACT

Numerical simulations were used to study mobilization and mixing of a bottom layer of Bingham liquid by agitating a Newtonian liquid above the Bingham layer. The agitation is done by a pitched-blade impeller at a Reynolds number of 6000. The Bingham liquid and the Newtonian liquid are miscible. The parameter space of the simulations has a yield stress number and a Richardson number as dimensionless variables. The yield stress number quantifies the importance of the yield stress relative to inertial stresses, the Richardson number the role of the density difference between the two liquids. The simulation procedure is based on the lattice-Boltzmann method for the flow dynamics, and a finite volume scheme to solve for the local and time dependent composition of the liquid mixture. Flow dynamics and liquid composition are intimately coupled. The moderate Reynolds number tentatively allows us to directly simulate the transitional flow, without a need for a turbulence closure model. The results quantify the increase of mixing time with increasing yield stress and (to a weaker extent) density difference.

1. Introduction

In this paper a specific – though not uncommon – situation is considered: a mixing tank that has been left un-agitated for some time has its contents segregated into a thick, paste-like layer on the bottom, and a lighter and less viscous portion of liquid above. The bottom layer is considered a Bingham liquid; the liquid above is supposed to be Newtonian. The research question is if turbulent agitation of the less viscous Newtonian phase is an efficient means to mobilize the Bingham liquid, and subsequently homogenize the tank contents. Obviously, many variables determine the answer to this question. The focus of the present study is on how the mixing process depends on the yield stress of the bottom layer. Also the effect of the density difference between the two liquids has been considered.

The situation as sketched above has been approached in a computational manner: we have attempted to mimic the mixing process by performing three-dimensional, time-dependent numerical simulations starting from a zero velocity and fully segregated state. The flow system poses a few interesting numerical challenges. In the first place we deal with turbulent flow, at least in the portion of the tank with Newtonian liquid. We do not, however, want to revert to turbulence modeling given the presence of the Bingham liquid and its (most likely) laminar flow character. Turbulence models usually are not designed and tested for accurately capturing (spatial or temporal) laminar-turbulent transitions. Not using turbulence models means that the flow needs to be fully resolved ("direct" simulations) which puts strong resolution demands. We mitigate these by considering a modest Reynolds number (Re = 6000 with Re precisely defined in the next section), and we check for grid effects, i.e. a significant number of cases that are physically identical have been performed on grids with different resolution. Also the discontinuous behavior of Bingham liquids (upon reaching the yield stress, zero deformation in the liquid switches to non-zero deformation) is a challenge for numerical methods.

Interesting flow physics is expected; not in the least given the turbulent nature of the flow "attacking" the Bingham layer. The average flow may be too weak to erode away the bottom Bingham layer, the intermittency of the turbulent flow emerging from the impeller may from time to time be sufficiently strong to locally overcome the yield stress and chip away some of the Bingham liquid. This will change the surface topology of the Bingham layer, making it rougher (more undulated) and therefore more susceptible for further erosion. With the gradual removal of the Bingham layer and associated changing bottom topology also the global structure of the flow of the Newtonian liquid gradually changes with time making this an interesting problem with a broad spectrum of time and length scales. Again adequate resolution of flow structures with high viscous and/or inertial stress is a key issue to realistically capture this process. It is anticipated that the density difference of the two liquids is not as important to the erosion process as the yield stress. For mixing the liberated Bingham material into the bulk flow, however, we do expect slower homogenization with increased density differences.

The nature of this work is quite specific, and I am not aware of similar studies in the literature. Closest comes the work by Frigaard and co workers [1–4] who studied displacement of wall

E-mail address: jos@ualberta.ca

0377-0257/$ - see front matter © 2012 Elsevier B.V. All rights reserved.
http://dx.doi.org/10.1016/j.jnnfm.2012.09.012

layers consisting of yield stress liquid by a Newtonian liquid. In their experiments and modeling work they mainly considered laminar flow in channels and pipes.

The aim of this paper in the first place is to quantify the homogenization of the initially segregated system. As in former papers [5,6], we use the decay of scalar variance in the stirred vessel as a means to monitor the mixing process and the time it takes to reach a certain low level of scalar variance as a measure for the mixing time. A wider ranging goal is to enhance our understanding as to how turbulent flow interacts with yield stress material. This goes beyond mixing tanks only. Examples of this nature are also encountered in fouling and removal of fouling in process equipment such as heat exchangers [7], or food processing devices, flow over biofilms [8], and sediment transport in slurry pipelines [9], to name only a few.

This paper is organized in the following manner: First the flow system and the liquid properties are described. Based on these, dimensionless numbers are defined, and the parameter range covered in this paper is identified. Subsequently the simulation procedure is outlined schematically with references to the literature for further details. We then present results. The emphasis will be on the effect of the yield stress on the mobilization of the Bingham layer. Conclusions are summarized in the last section.

2. Flow systems

There are two liquids present in the tank: a Newtonian liquid with density ρ_N and dynamic viscosity $\rho_N\nu$, and a Bingham liquid with density ρ_B (with $\rho_B \geqslant \rho_N$), yield stress τ_Y and plastic (dynamic) viscosity $\rho_B\nu$. This implies that the two liquids share the same kinematic viscosity ν; we made this choice to limit the dimensions of the parameter space that we want to cover in this study.

The tank and agitator, and the coordinate system as used in this work are shown in Fig. 1. The tank is cylindrical with four equally spaced baffles along its perimeter that are placed there to prevent solid body rotation of the liquid and thus enhance mixing. The flow is driven by four pitched (45°) blades attached to a hub that is mounted on a shaft that enters through the top of the tank. The tank is closed off with a lid so that at the top surface (as on all other solid surfaces) a no-slip condition applies. The Reynolds number of this flow system is defined as $\mathrm{Re} = \frac{ND^2}{\nu}$, with N the impeller speed (in rev/s), and D the impeller diameter. The impeller is operated in the down-pumping mode.

The yield stress gives rise to an additional dimensionless number, and so does the density difference between the two liquids. A yield stress number Y is defined as $Y = \frac{\tau_Y}{\rho_N N^2 D^2}$. Given the turbulent (i.e. inertial) nature of the flow that is designated to erode the Bingham liquid layer we have chosen to equate τ_Y with a measure for the inertial stress in the mixing tank $\rho_N N^2 D^2$, not with a viscous stress. This explains the use of ρ_N (and not for instance the average density) in the expression for Y. Density differences and buoyancy have been quantified through a Richardson number $\mathrm{Ri} = \frac{g(\rho_B - \rho_N)}{\bar{\rho} N^2 D}$. In the Richardson number g is gravitational acceleration, and $\bar{\rho}$ is the tank-averaged liquid density.

The simulations start from a stable stratification and zero liquid velocity everywhere with the heavier Bingham liquid forming a layer on the bottom with thickness $H = T/6$. With this initial condition the impeller is initially fully surrounded by the (lighter) Newtonian liquid. At moment $t = 0$ the impeller is started and from then on has a constant angular velocity $2\pi N$ (rad/s).

The local composition of the liquid is represented by a scalar field c (with $c = 1$ pure Newtonian liquid; $c = 0$ pure Bingham liquid) for which we solve a transport equation

$$\frac{\partial c}{\partial t} + u_i \frac{\partial c}{\partial x_i} = \Gamma \frac{\partial^2 c}{\partial x_i^2} \tag{1}$$

(summation over repeated indices) with u_i the ith component of the fluid velocity vector. The two liquids are miscible and have a mutual diffusion coefficient Γ which (in a dimensionless sense) has been represented by the Schmidt number $\mathrm{Sc} \equiv \frac{\nu}{\Gamma}$. For the local mixture density a linear relationship with c is assumed: $\rho_{mix} = \rho_B + c(\rho_N - \rho_B)$. Buoyancy has been incorporated via a Boussinesq approximation: a liquid element having density ρ_{mix} feels a body force in positive z-direction (as defined in Fig. 1) of $f_z = g(\bar{\rho} - \rho_{mix})$. In the Boussinesq approximation, the body force term is the only place where the density variation enters the Navier–Stokes equations. This approximation limits the density differences that can be simulated; for the approximation to be valid $\frac{(\rho_B - \rho_N)}{\bar{\rho}} \ll 1$ (that is $\mathrm{Ri} \ll \frac{g}{N^2 D}$) is required. The mixture yield stress is assumed to be a step function of the liquid composition:

$$\tau_{Y,mix} = \tau_Y \quad \text{if } c \leqslant 0.5; \quad \tau_{Y,mix} = 0 \quad \text{if } c > 0.5. \tag{2}$$

As mentioned above, the two liquids share the same (plastic) kinematic viscosity.

Of the four dimensionless groups identified (Re, Y, Ri, Sc), two (Y and Ri) have been varied, the other two (Re and Sc) were kept constant. The Reynolds number was fixed to Re = 6000. With this Reynolds number we feel confident of doing well-resolved turbulence

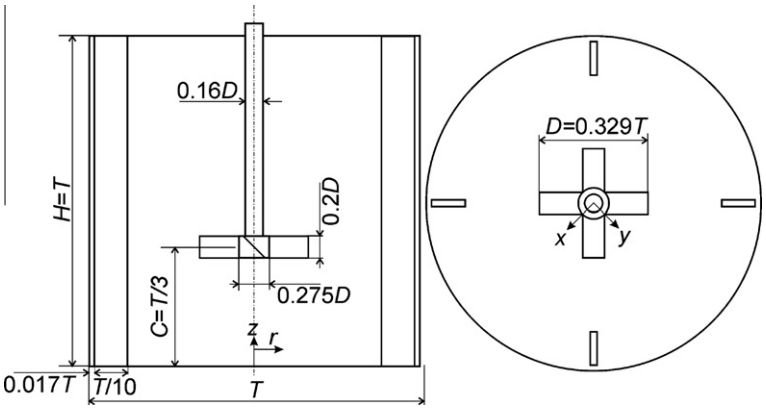

Fig. 1. The stirred tank geometry considered: a baffled tank with a pitched-blade impeller mounted on a shaft that enters the tank through the top. The coordinate systems ((r,z) and (x,y,z)) are fixed and have their origin in the center at the bottom of the tank. The top of the tank is closed off with a lid. The impeller rotates such that it pumps liquid down.

simulations on fairly modest grids [5]. This allows running a significant number of cases for a sufficient number of impeller revolutions per simulation case. We do not expect the Schmidt number to strongly influence the flow physics, as long as it is "large", i.e. the transport of scalar c is dominated by convection, much less by diffusion. In this study Sc = 1000. In the next section (on the numerical approach) this value will be interpreted in the light of additional numerical diffusion.

The Richardson number has been varied in the range $0 \leqslant \mathrm{Ri} \leqslant 0.5$. Previous simulations on mixing of Newtonian liquids with density differences [5] point at strongly increased mixing times (by a factor of up to 6) for the higher end of this Ri-range. The yields stress number was in the range $0 \leqslant Y \leqslant 0.8$. To interpret this range of Y, we revert to the physical system of a lab-scale mixing tank with diameter $T = 0.3$ m, filled with a moderately viscous Newtonian liquid with $\nu_N = 10^{-5}$ m^2/s and $\rho_N = 1000$ kg/m^3. In order to achieve Re = 6000, the impeller speed is $N = 6$ rev/s. Then $Y = 0.8$ (the largest value of Y considered) implies $\tau_Y \approx 300$ N/m^2.

3. Modeling approach

The lattice-Boltzmann method (LBM) has been applied to numerically solve the incompressible flow equations [10,11]. Lattice-Boltzmann fluids can be viewed as collections of (fictitious) fluid particles moving over a regular lattice, and interacting with one another at lattice sites. These interactions (collisions) give rise

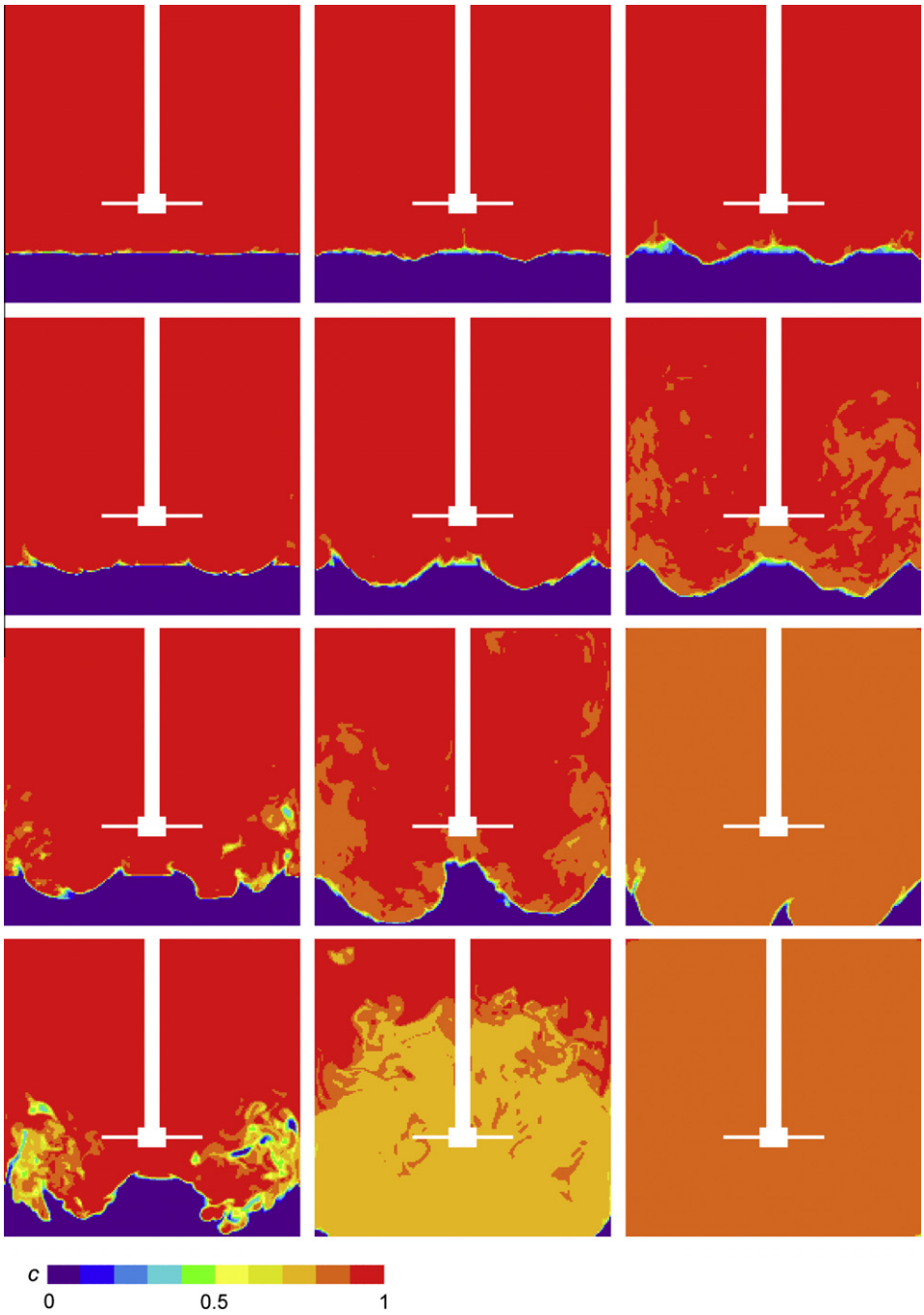

Fig. 2. Instantaneous realizations of the scalar concentration in the mid-baffle plane at $tN = 5$, 25, and 100 (left to right), and for $Y = 0.025$, 0.1, 0.2, and 0.8 (bottom to top). Ri = 0.25.

to viscous behavior of the fluid, just as colliding/interacting molecules do in real fluids. The main reasons for employing the LBM for fluid flow simulations are its computational efficiency and its inherent parallelism, both not being hampered by geometrical complexity. Lattice-Boltzmann approaches are gaining traction in applications involving non-Newtonian liquids [12–16].

The basis for the LBM formulation as used in this paper has been put forward by Somers [17], also see [18]. It falls in the category of three-dimensional, 18 speed (D3Q18) models. Its grid is uniform and cubic. In order to allow for Bingham rheology, the Somers-scheme has been extended with a stress formulation as the one Vikhansky [13] proposed for lattice-Boltzmann schemes. In the Somers-scheme, the collision operation is formulated in terms of the primitive flow variables density ρ (which is equivalent to pressure via an equation of state), momentum ρu_i, and deviatoric stress τ_{ij}. In the collision operation first the magnitude of the stress $|\tau| \equiv \sqrt{\frac{1}{2}\tau_{ij}\tau_{ij}}$ is determined. If for a certain location and time instant $|\tau| < \tau_{Y,mix}$, the liquid is locally unyielded and the deformation tensor $d_{ij} = \frac{1}{2}\left(\frac{\partial u_j}{\partial x_i} + \frac{\partial u_i}{\partial x_j}\right)$ is set explicitly to zero in the collision operation. If on the other hand $|\tau| \geqslant \tau_{Y,mix}$, the apparent viscosity can be determined: $\nu_a = \nu + \frac{\tau_{Y,mix}}{\dot{\gamma}\rho_{mix}}$ with the now non-zero $\dot{\gamma} = \sqrt{2d_{ij}d_{ij}}$, and we proceed with a normal (viscous) collision operation according to the apparent viscosity ν_a. It is important to note that this is not a viscosity regularization approach [4]. In the latter, the unyielded part of the Bingham rheology is approximated by a very high (however finite) viscosity. Regularization introduces this zero-shear viscosity as an arbitrary numerical parameter and (therefore) allows for finite deformation for essentially unyielded liquid. These are undesirable features [4].

Vikhansky [13] showed that his procedure provides excellent agreement with analytical results for planar channel flow. He also compared results for more complex flow systems with finite element solutions again showing favorable agreement. In addition to two variants of planar channel flow, we performed simulations of two-dimensional lid-driven cavity flow and compared results to the numerical results due to Yu and Wachs [19], that were based on a finite difference based projection method. Results of our benchmarks are detailed in Appendix A and convincingly show that Bingham rheology is well represented by the numerical procedure.

In the LBM, planar no-slip walls naturally follow when applying the bounce-back condition [11]. For non-planar and/or moving walls (that we have since we are simulating the flow in a cylindrical, baffled mixing tank with a revolving impeller) an adaptive force field technique (a.k.a. immersed boundary method) has been used [20,21].

We solve the transport equation in the liquid composition c (Eq. (1)) with an explicit finite volume discretization on the same (uniform and cubic) grid as the LBM. A clear advantage of employing a

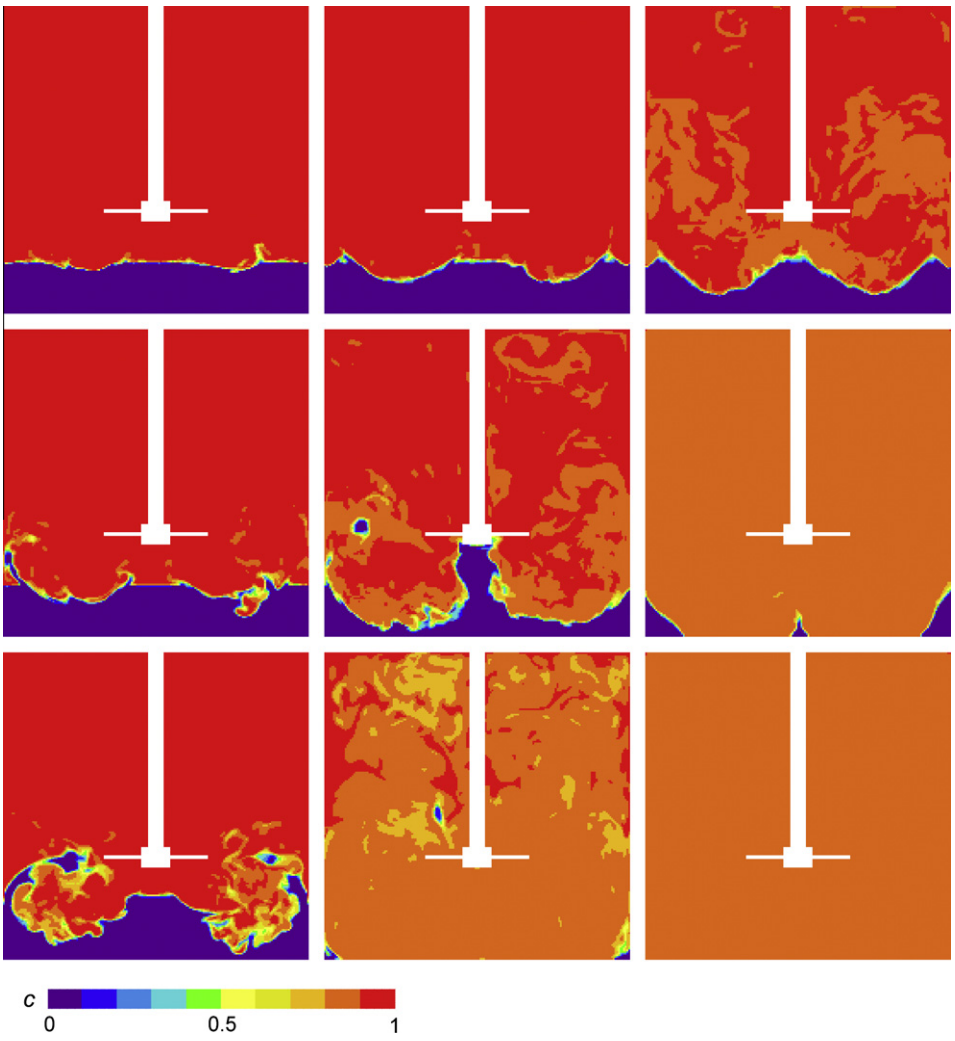

Fig. 3. Instantaneous realizations of the scalar concentration in the mid-baffle plane at tN = 5, 25, and 100 (left to right), and for Y = 0.025, 0.1, and 0.2 (bottom to top). Ri = 0.0.

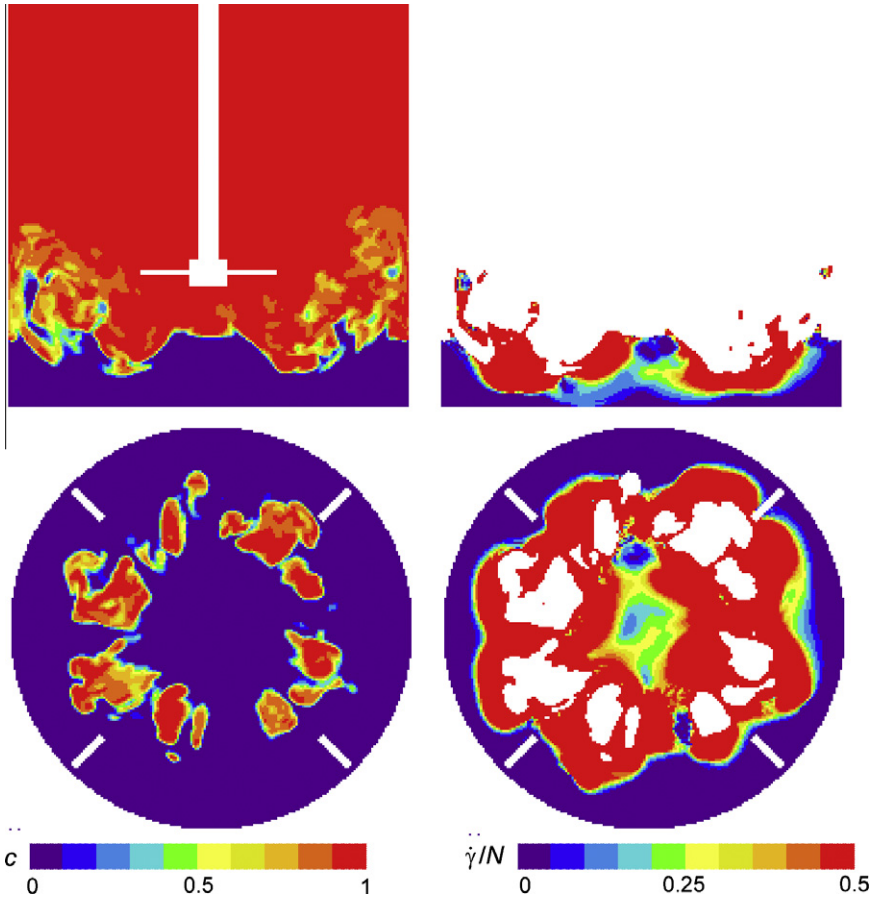

Fig. 4. Instantaneous realizations of concentration field cross sections (left) and deformation rate in the Bingham portion of the liquid (right) for the case with $Y = 0.05$ and $\mathrm{Ri} = 0.25$ at $t\mathrm{N} = 5$.

finite volume formulation is the availability of methods for suppressing numerical diffusion. As in previous works [22,23], TVD discretization with the Superbee flux limiter for the convective fluxes [24,25] was employed. We step in time according to an Euler explicit scheme. This explicit finite volume formulation for scalar transport does not hamper the parallelism of the overall numerical approach.

The large value (10^3) of the Schmidt number makes the micro-scalar-scales (Batchelor scale) a factor of $\sqrt{\mathrm{Sc}} \approx 30$ smaller than the Kolmogorov length scale and quite impossible to resolve in our numerical simulations. In the simulations – although we as much as possible suppress numerical diffusion – diffusion will be controlled by the grid spacing and the precise value of Sc based on molecular diffusivity Γ will have marginal impact on the computational results. In order to assess to what extent numerical diffusion influences the outcomes of our simulations, grid effects have been assessed and will be discussed later in the paper.

It is emphasized here that the scalar concentration field c is two-way coupled to the flow field, i.e. c is advected by the flow (see u_i in Eq. (1)) and at the same time it affects the flow since c determines the local yield stress (Eq. (2)) and the local density of the liquid mixture that in turn determines the (net) gravity force locally felt by the liquid.

3.1. Numerical settings

Given $\mathrm{Re} = 6000$ we expect mildly turbulent flow in the Newtonian part of the mixing tank. The micro-scale of turbulence (Kolmogorov length scale η) relates to a macroscopic length scale (say the tank diameter T) according to $\eta = T\mathrm{Re}^{-\frac{3}{4}}$. The criterion for sufficiently resolved direct numerical simulations of turbulence is $\Delta < \pi\eta$ [26,27]. Our default grid is such that the tank diameter is spanned by 180 lattice spacings: $T = 180\Delta$. According to the above resolution criterion, this grid slightly under-resolves the flow ($\pi\eta \approx 0.8\Delta$). As discussed above, full resolution of the Bachelor scale (η_B) is not an option as it is a factor of 30 smaller than the Kolmogorov scale. The consequences of not fully resolving η, and not resolving η_B have been assessed through grid refinement: A number of simulations have been performed on a finer grid with $T = 330\Delta$. In addition, in previous work [6] on mixing of Newtonian liquids a more extensive grid study (with grids up to $T = 552\Delta$) was performed at Reynolds and Schmidt numbers and in a geometry comparable to the present one. There we observed an effect (albeit weak) of grid resolution on scalar mixing time: from the coarsest $T = 180\Delta$ grid to the finest $T = 552\Delta$ grid, mixing times differed by 10% at maximum.

The number of time steps to complete one impeller revolution is 2000. In this manner the tip speed of the impeller is $\pi ND = 0.094$ in lattice units (with the impeller diameter $D = T/3$) which keeps the flow velocities in the tank well below the speed of sound of the lattice-Boltzmann system thus achieving incompressible flow. Due to the explicit nature of the lattice-Boltzmann method and its (in)compressibility constraints, the finer grid with $T = 330\Delta$ requires more time steps per impeller revolution: 3600.

4. Results

4.1. Flow and scalar field impressions

The qualitative discussion of the results of our simulations first focuses on the vertical plane through the center of the tank, in

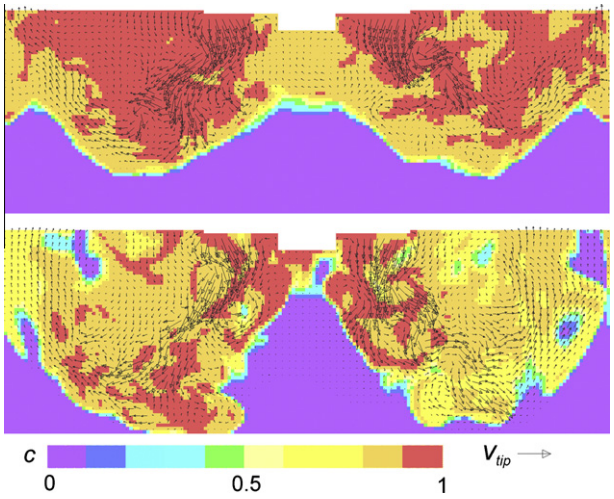

Fig. 5. Instantaneous realizations of the scalar concentration overlaid with velocity vectors in the part of the mid-baffle plane below the impeller. Two typical situations. Top: $Y = 0.2$ and Ri = 0.25 at $tN = 100$. Bottom: $Y = 0.05$ and Ri = 0.25 at $tN = 10$. Resolution is $T = 180\Delta$; the resolution of the simulation is twice as high in each direction as the resolution of the velocity vector field shown.

between two baffles (the *xz*-plane in the coordinate system defined in Fig. 1). We show velocity vector fields, contours of liquid composition *c*, and contours of liquid deformation $\dot{\gamma}$ in this plane. As the default Richardson number we chose Ri = 0.25.

The way the concentration field *c* in the *xz*-plane evolves in time is shown in Fig. 2 for four different values of *Y*. It shows – as expected – that the impact of *Y* on the mobilization and mixing of the Bingham layer is profound. Mobilization of the bottom Bingham layer gets increasingly harder with increasing *Y*. Previous work [5] on Newtonian liquid mixing with density differences suggests a time to homogenization (this "mixing time" has been defined in detail in [5]) at Ri = 0.25 and Re = 6000 of 140 impeller revolutions. Fig. 2 shows that homogenization times of such order are to be expected for $Y = 0.025$ as well; for higher values of *Y* mixing gets much slower and for $Y = 0.8$ the Bingham layer is not mobilized (let alone mixed) at all. At this high value of *Y* the primary effect of the turbulent Newtonian liquid flow above the Bingham layer is an indentation of the top surface of the layer there where the downward stream emerging from the impeller hits it. The depth of the indentation slowly increases in time. A secondary effect of the Newtonian liquid flow is some erosion of Bingham liquid as a result of a shear flow of Newtonian liquid over the interface with the Bingham liquid. This erosion gets more traction with the increase of the dents with time. The processes (indentation and erosion) are similar (albeit stronger) for $Y = 0.2$. True mobilization (i.e. significant flow) of the Bingham layer only occurs if $Y \leqslant 0.1$. The physical picture hardly changes if the Richardson number is reduced from Ri = 0.25 to Ri = 0; compare Figs. 3 and 2. This suggests that the yield stress dominates gravity-induced stresses in the mobilization process. This is not necessarily obvious given that gravity-stress is definitely not negligible compared to

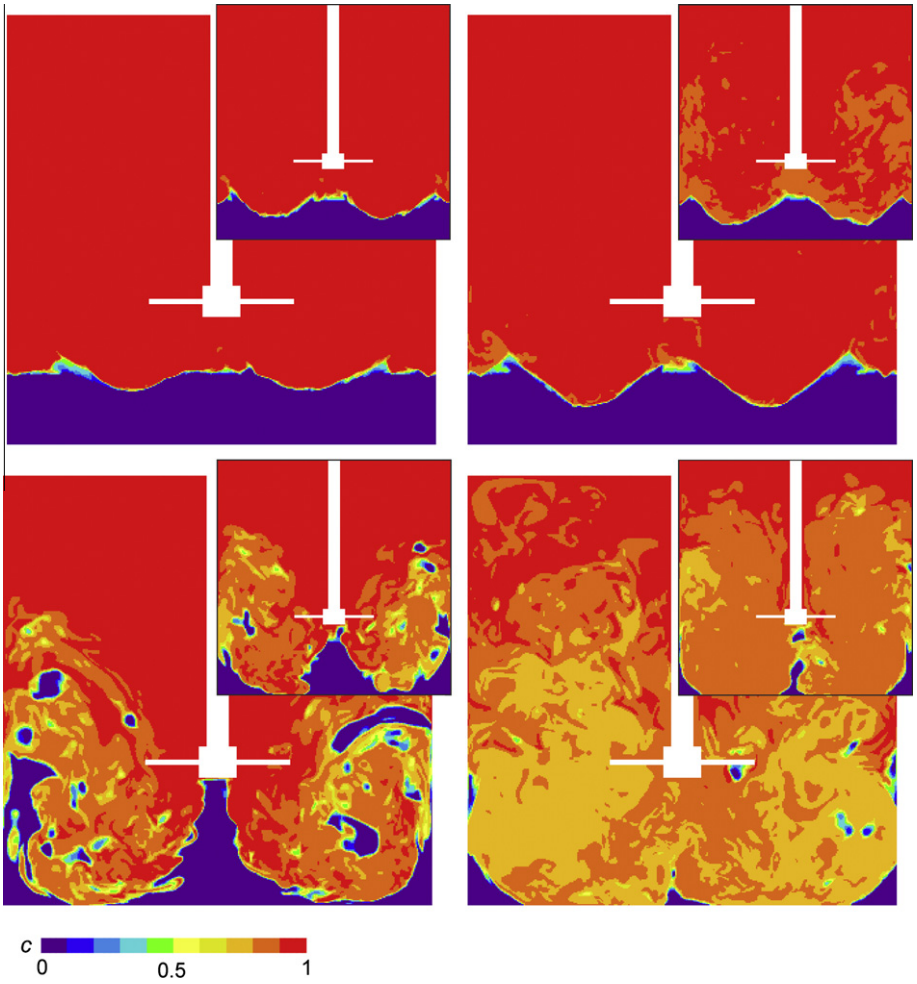

Fig. 6. Instantaneous realizations of the scalar concentration in the mid-baffle plane; qualitative comparison between grids. Each large panel has $T = 330\Delta$; each inset has $T = 180\Delta$. Top row: $Y = 0.2$ and Ri = 0.25 at $tN = 25$ (left), and 100 (right). Bottom row: $Y = 0.05$ and Ri = 0.25 at $tN = 10$ (left) and 20 (right).

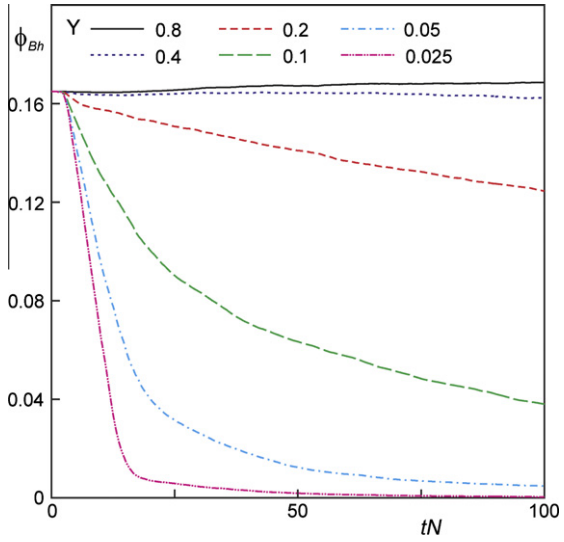

Fig. 7. Time series of the volume fraction Bingham liquid ϕ_{Bh} for various Y (as indicated) at Ri = 0.25. Resolution is $T = 180\Delta$.

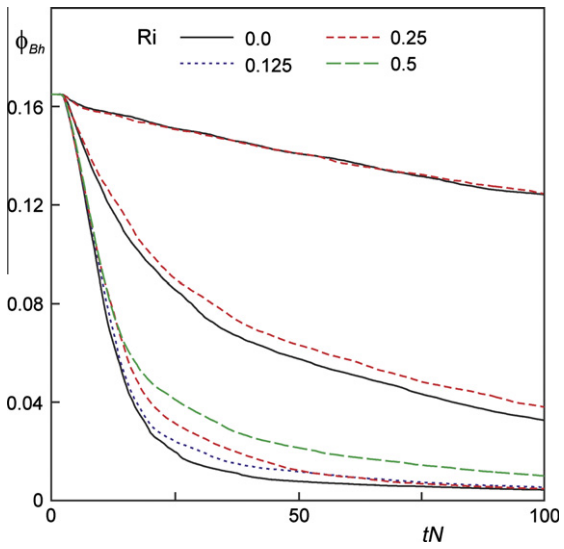

Fig. 8. Time series of the volume fraction Bingham liquid ϕ_{Bh}. Effect of the Ri as indicated. The three groups of curves have (from highest to lowest) $Y = 0.2$, 0.1, and 0.05. Resolution is $T = 180\Delta$.

yield stress: $\frac{g\Delta\rho D}{\tau_Y} \approx \frac{\mathrm{Ri}}{Y} \geqslant 0.3$ for all cases shown in Fig. 2 (that all have Ri = 0.25).

The three-dimensional nature and the level of detail contained in the simulations are illustrated in Fig. 4. In addition to concentration fields the figure shows deformation levels in the Bingham portions of the liquid. The horizontal cross sections show the influence of the impeller and the baffles at the perimeter of the tank on the structure of the liquid mixture. As can be seen, the baffles help sustain for some time a layer of essentially unyielded liquid at the perimeter of the tank. The impeller pumps down Newtonian liquid and creates strong deformation so that Bingham liquid first gets replaced by Newtonian liquid underneath the impeller blades. That the concentration field c is truly two-way coupled with the flow dynamics is shown in Fig. 5. In that figure we combine concentration contours with velocity vectors. It shows a strong flow above, and virtually no flow inside the Bingham layer.

In a qualitative sense, the refined grid with $T = 330\Delta$ does not seem to display significantly more or fundamentally different

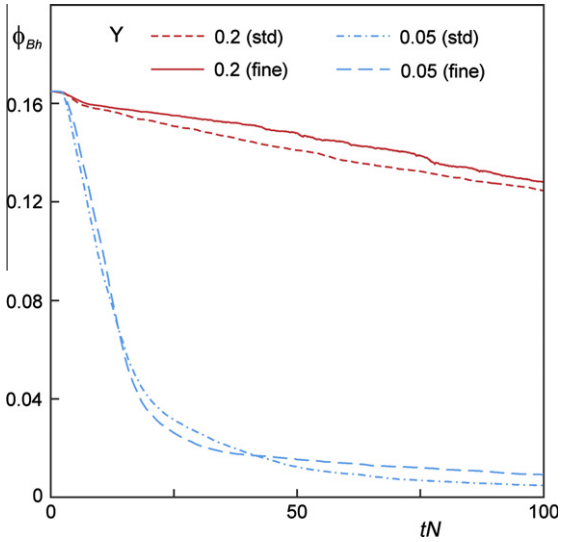

Fig. 9. Time series of the volume fraction Bingham liquid ϕ_{Bh} for two values of Y (as indicated) at Ri = 0.25. Effects of spatial resolution of the simulations: $T = 180\Delta$ (standard = std); $T = 330\Delta$ (fine).

features compared to the standard grid of $T = 180\Delta$, see Fig. 6. The results for $Y = 0.05$ in Fig. 6, however, hint at the finer grid being able of capturing more small pockets of Bingham liquid dispersed in the Newtonian phase after they got detached from the bottom layer. Results on different grids will be compared quantitatively in the next section.

4.2. Mobilization and mixing time analyses

To quantitatively compare different physical and numerical (grids) cases we monitor the evolution of the amount of Bingham liquid (liquid having $c \leqslant 0.5$) in the tank. Most simulations were run over 100 impeller revolutions after start-up from the zero-velocity and fully stratified initial condition. Fig. 7 compares case with different yield stress number Y at a fixed Richardson number of Ri = 0.25. A clear decay only occurs if $Y \leqslant 0.2$. If $Y = 0.4$ the amount of Bingham liquid stays virtually constant over the time period of 100 revolutions; if $Y = 0.8$ the total amount of Bingham liquid even slightly increases. The latter is the result of the formation of a thin erosion boundary layer above the Bingham bottom layer with in the lower portion of the boundary layer $c \leqslant 0.5$. Fig. 7 also shows that only for $Y \leqslant 0.05$ the Bingham layer gets removed within 100 impeller revolutions. For three of the time series in Fig. 7 ($Y = 0.2$, 0.1, and 0.05) we show in Fig. 8 that buoyancy has only slight impact on the mobilization process. The minor trends with respect to Ri follow our intuition: a larger Ri (i.e. a larger density difference between the liquids) slows down the removal of the Bingham layer.

In Fig. 9 a weak grid dependency is observed with on average a little less decay of the amount of Bingham liquid for the finer ($T = 330\Delta$) grid. This is in line with the observation in Fig. 6 where it was noticed that portions of Bingham liquid removed from the bottom layer and traveling through the bulk of the tank were better resolved on the finer grid.

Homogenization of the tank contents not only requires deforming and mobilizing the Bingham layer. Once mobilized the Bingham liquid needs to get mixed with the rest of the tank content. As in previous papers [5,6], we have quantified homogenization by observing the scalar concentration variance in a vertical plane (the xz plane) as a function of time: $\sigma^2(t) = \frac{1}{A}\iint_A \left[c^2(x, y = 0, z, t) - (\langle c \rangle(t))^2\right] dxdz$ with $\langle c \rangle(t)$ the average scalar concentration in the mid-baffle plane at

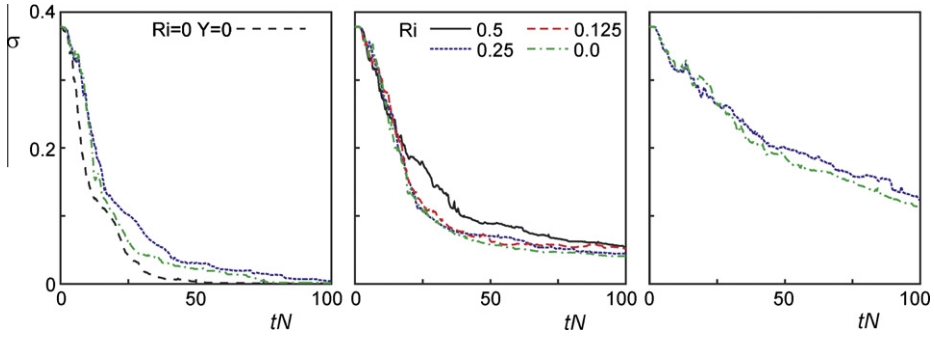

Fig. 10. Scalar variance σ in the xz-plane as a function of time. From left to right: $Y = 0.025$, 0.05, and 0.1. Ri as indicated. For reference the decay of σ for a single-liquid Newtonian system ($Y = 0$ and Ri = 0) has been given.

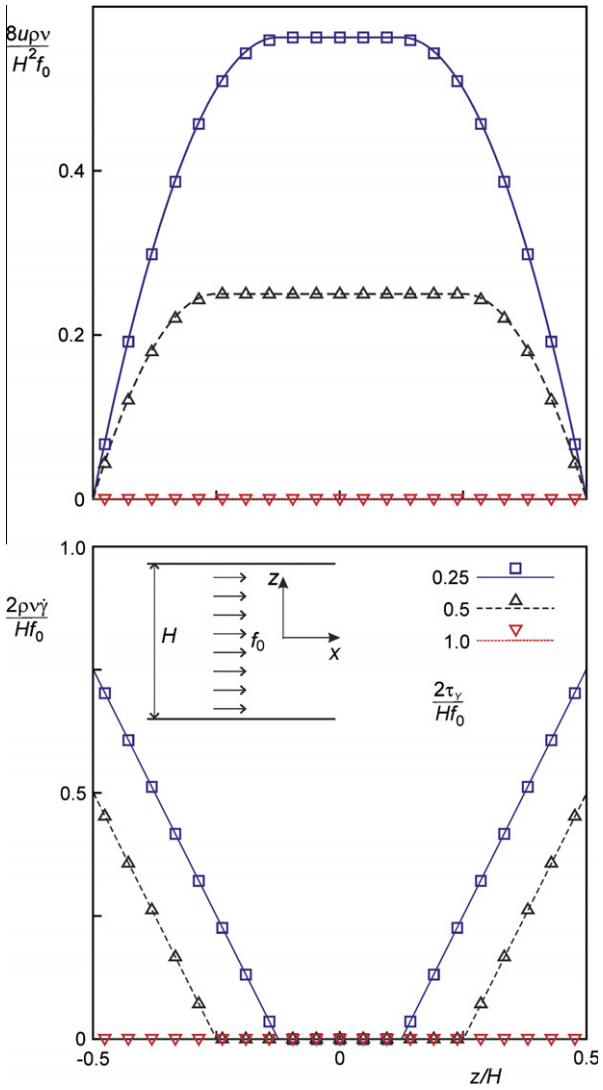

Fig. A1. One-dimensional channel flow driven by a body force f_0 in the positive x-direction (see the inset in the lower panel). Top: velocity in x-direction u as a function of z for $\frac{2\tau_Y}{Hf_0} = 0.25, 0.5$, and 1.0 (as indicated). Bottom: $\dot{\gamma}$ (which is $\frac{\partial u}{\partial z}$ for this one-dimensional flow) as a function of z. Symbols: numerical solution; lines: analytical solution.

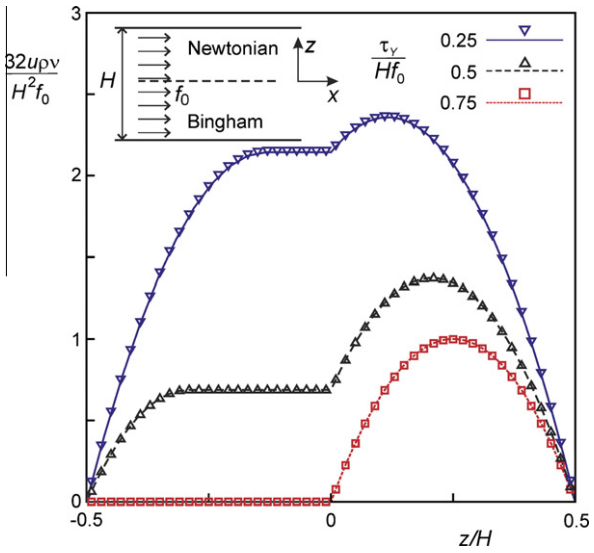

Fig. A2. One-dimensional channel flow with Bingham liquid in the bottom half ($-H/2 \leqslant z \leqslant 0$) and Newtonian liquid in the top half ($0 \leqslant z \leqslant H/2$). The flow is driven by a body force f_0 in the positive x-direction (see the inset). Velocity in x-direction u as a function of z for $\frac{\tau_Y}{Hf_0} = 0.25, 0.5$, and 0.75 (as indicated). Symbols: numerical solution; lines: analytical solution.

moment t. At time zero the liquids are fully segregated with $c = 1$ in the upper 5/6th of the cross section, and $c = 0$ in the lower 1/6th, and $\langle c \rangle(t = 0) = 5/6$ so that the starting value of the standard deviation is $\sigma(t = 0) = \sqrt{5}/6 \approx 0.373$. The decay of σ as a function of Y and Ri is shown in Fig. 10. For reference we show in the left panel of Fig. 10 how σ would decay if the tank was filled with a single Newtonian liquid that was tagged with a passive scalar concentration $c = 0$ in the $T/6$ bottom layer and $c = 1$ in the rest of the tank. Comparison with the reference case shows that non-zero Y and Ri slow down the mixing process. This effect is minor for $Y = 0.025$ (Fig. 10, left panel) but gets progressively stronger for increasing Y and Ri. As already observed when analyzing the decay of the amount of Bingham liquid, the dominant parameter is Y.

5. Summary

This paper discussed the practically relevant, though quite specific situation of mobilization and mixing of a layer of Bingham liquid at the bottom of a mixing tank through agitation with an impeller of Newtonian liquid above. The two liquids have been considered miscible. The main dependencies that have been investigated relate to the yield stress of the Bingham liquid, and the density difference between the Bingham liquid and the Newtonian liquid. The yield stress has been non-dimensionalized through the group $Y = \frac{\tau_Y}{\rho_N N^2 D^2}$, the density difference through a Richardson number $\mathrm{Ri} = \frac{g(\rho_B - \rho_N)}{\bar{\rho} N^2 D}$. In addition to Y and Ri, the flow problem is

Fig. A3. Lid-driven cavity flow as defined in the left panel. The contour plots are for Bn = 5, 20, and 50 (left to right). Black indicates $\dot{\gamma} = 0$ (i.e. unyielded); white indicates $\dot{\gamma} \geqslant 0.01u_0/H$; the in-between grey scale is linear. Re = 0.05.

defined by the tank's and impeller's geometrical layout, an impeller Reynolds number $\mathrm{Re} = \frac{ND^2}{\nu}$ and the Schmidt number $\mathrm{Sc} = \frac{\nu}{\Gamma}$. Geometry, Re, and Sc were constant in this study, with Re = 6000 indicating weakly turbulent flow in the Newtonian portion of the tank, and Sc = 1000 which is typical for diffusion in liquids. The tank layout involved a pitched-blade impeller and a baffled tank.

The approach to this problem was purely computational. We solve the three-dimensional, time dependent flow in the tank by means of the lattice-Boltzmann method that was equipped with Bingham rheology according to an approach due to Vikhansky [13]. In addition a transport equation for an active scalar concentration c that represents the (local and time dependent) composition of the liquid in the tank has been solved. For the latter a finite volume method was used.

This hybrid LB/FV method provides an efficient numerical procedure that allows for (at this modest Reynolds number) sufficient resolution of the flow dynamics and for running long time series (typically 100 impeller revolutions starting from a quiescent stably stratified state) so as to monitor the mixing process. However, the high Schmidt number makes that we do not resolve the finest scalar length scales. This issue has been dealt with in a heuristic manner by studying the effect of grid refinement on the mixing process. The observed grid effects are relatively weak and thereby suggest that full resolution of the scalar field is not critical for the global behavior of the flow system.

The simulations provide a detailed view of the mobilization of the Bingham liquid and the way it gets mixed with the Newtonian liquid. If Y exceeds 0.4, the Newtonian liquid is unable to mobilize the Bingham layer. If $Y = 0.025$ the Bingham rheology is hardly felt and the liquids mix almost as fast as a Newtonian liquid mixture would. In between these two values the length of the homogenization process is a strong function of Y, and to a lesser extent of Ri.

This work clearly needs experimental validation. Ideally such experiments aim at directly observing the mixing process inside the tank by means of e.g. laser sheet visualization. It may be a challenge to select sufficiently transparent liquids having the desired rheological behavior for this. The simulation procedure is, however, not restricted to the precise rheology as described in the current paper. It would for instance be very well possible to implement Herschel–Bulkley rheology in the computer code.

Appendix A

A.1. Benchmark 1: planar channel

We consider the laminar flow driven by a body force f_0 of Bingham liquid between two parallel flat plates a distance H apart (see the inset in Fig. A1). The liquid has a yield stress τ_Y and a plastic viscosity $\rho\nu$. In the numerical solution H has been discretized by 21 lattice spacings Δ. In Fig. A1 numerical results for velocity and deformation rate are compared with the analytical solution for three values of the yield stress. If $\frac{2\tau_Y}{Hf_0} \geqslant 1$ the body force cannot mobilize the liquid; for $\frac{2\tau_Y}{Hf_0} < 1$ it can. Numerical and analytical results are in good agreement.

A.2. Benchmark 2: one-dimensional layered channel

Since we have a Bingham liquid and a Newtonian liquid in the mixing tank we here consider the similar but much simpler situation of a layered laminar channel flow (see Fig. A2). The flow is again driven by a body force f_0 and the channel has a width H. The lower half of the channel contains the Bingham liquid with yield stress τ_Y and a plastic viscosity $\rho\nu$; the upper half contains Newtonian liquid with dynamic viscosity $\rho\nu$. As long as $\tau_Y \geqslant 0.75Hf_0$ the Bingham liquid is not yielded and the Newtonian liquid sees it as a solid wall. This gives rise to a parabolic profile in the Newtonian part of the channel with maximum velocity $\frac{f_0H^2}{32\rho\nu}$. For $\tau_Y < 0.75Hf_0$ the Bingham liquid gets yielded, starting at the wall.

In Fig. A2 numerical solutions on a grid such that $H = 50\Delta$ are compared with analytical solutions. The agreement between analytical and numerical results is very good. It is particularly encouraging to see that the Bingham liquid stays unyielded at the demarcation point $\tau_Y = 0.75Hf_0$.

A.3. Benchmark 3: two-dimensional lid-driven cavity

Consider the two-dimensional flow in a square lid-driven cavity with side length H and top-wall velocity u_0 in the positive x-direction (see Fig. A3). For this flow we define the Bingham number as $\mathrm{Bn} = \frac{\tau_Y H}{\rho\nu u_0}$, and the Reynolds number as $\mathrm{Re} = \frac{u_0 H}{\nu}$. The spatial resolution is such that $H = 161\Delta$. In Fig. A2 we show this flow in terms of the unyielded and yielded portions of the liquid (in a view inspired by Yu and Wachs [19]) for three values of Bn. These results can be directly compared to results in [19] (their Fig. 3). Good agreement is observed.

References

[1] S.M. Taghavi, K. Alba, M. Moyers-Gonzalez, I.A. Frigaard, Incomplete fluid–fluid displacement of yield stress fluids in near-horizontal pipes: experiments and theory, J. Non-Newton. Fluid Mech. 167 (2012) 59.
[2] S. Hormozi, K. Wielage-Burchard, I.A. Frigaard, Entry, start up and stability effects in visco-plastically lubricated pipe flows, J. Fluid Mech. 673 (2011) 432.
[3] K. Wielage-Burchard, I.A. Frigaard, Static wall layers in plane channel displacement flows, J. Non-Newton. Fluid Mech. 166 (2011) 245.
[4] M. Allouche, I.A. Frigaard, G. Sona, Static wall layers in the displacement of two visco-plastic fluids in a plane channel, J. Fluid Mech. 424 (2000) 243.
[5] J.J. Derksen, Blending of miscible liquids with different densities starting from a stratified state, Comput. Fluids 50 (2011) 35.
[6] J.J. Derksen, Direct simulations of mixing of liquids with density and viscosity differences, Ind. Eng. Chem. Res. 51 (2012) 6948.
[7] E.A. Ishiyama, F. Coletti, S. Macchietto, W.R. Paterson, D.I. Wilson, Impact of deposit ageing on thermal fouling: lumped parameter model, AIChE J. 561 (2010) 531.
[8] C. Picioreanu, J.-U. Kreft, M.C.M. van Loosdrecht, Particle-based multidimensional multispecies biofilm model, Appl. Environ. Microbiol. 70 (2004) 3024.
[9] K.C. Wilson, R.S. Sanders, R.G. Gillies, C.A. Shook, Verification of the near-wall model for slurry flow, Powder Technol. 197 (2010) 247.

[10] S. Chen, G.D. Doolen, Lattice Boltzmann method for fluid flows, Annu. Rev. Fluid Mech. 30 (1998) 329.
[11] S. Succi, The Lattice Boltzmann Equation for Fluid Dynamics and Beyond, Clarondon Press, Oxford, 2001.
[12] I. Ginzburg, K. Steiner, A free-surface lattice-Boltzmann method for modeling the filling of expanding cavities by Bingham fluids, Philos. Trans. Roy. Soc. Lond. A 360 (2002) 453.
[13] A. Vikhansky, Lattice-Boltzmann method for yield-stress liquids, J. Non-Newton. Fluid Mech. 155 (2008) 95.
[14] J.J. Derksen, Prashant, simulations of complex flow of thixotropic liquids, J. Non-Newton. Fluid Mech. 160 (2009) 65.
[15] O. Malaspinasa, N. Fiétier, M. Deville, Lattice Boltzmann method for the simulation of viscoelastic fluid flows, J. Non-Newton. Fluid Mech. 165 (2010) 1637.
[16] N. Goyal, J.J. Derksen, Direct simulations of spherical particles sedimenting in viscoelastic fluids, J. Non-Newton. Fluid Mech., in press, http://dx.doi.org/10.1016/j.jnnfm.2012.07.006.
[17] J.A. Somers, Direct simulation of fluid flow with cellular automata and the lattice-Boltzmann equation, Appl. Sci. Res. 51 (1993) 127.
[18] J.G.M. Eggels, J.A. Somers, Numerical simulation of free convective flow using the lattice-Boltzmann scheme, Intl. J. Heat Fluid Flow 16 (1995) 357.
[19] Z. Yu, A. Wachs, A fictitious domain method for dynamic simulation of particle sedimentation in Bingham fluids, J. Non-Newton. Fluid Mech. 145 (2007) 78.
[20] D. Goldstein, R. Handler, L. Sirovich, Modeling a no-slip flow boundary with an external force field, J. Comput. Phys. 105 (1993) 354.
[21] J. Derksen, H.E.A. Van den Akker, Large-eddy simulations on the flow driven by a Rushton turbine, AIChE J. 45 (1999) 209.
[22] H. Hartmann, J.J. Derksen, H.E.A. Van den Akker, Mixing times in a turbulent stirred tank by means of LES, AIChE J. 52 (2006) 3696.
[23] J.J. Derksen, Scalar mixing by granular particles, AIChE J. 54 (2008) 1741.
[24] P.K. Sweby, High resolution schemes using flux limiters for hyperbolic conservation laws, SIAM J. Numer. Anal. 21 (1984) 995.
[25] Y. Wang, K. Hutter, Comparisons of numerical methods with respect to convectively dominated problems, Int. J. Numer. Meth. Fluids 37 (2001) 721.
[26] P. Moin, K. Mahesh, Direct numerical simulation: a tool in turbulence research, Annu. Rev. Fluid Mech. 30 (1998) 539.
[27] V. Eswaran, S.B. Pope, An examination of forcing in direct numerical simulations of turbulence, Comput. Fluids 16 (1988) 257.